American Journal of Pathology, Vol. 165, No. 6, December 2004

Vascular Biology, Atherosclerosis and Endothelium Biology

Dysmorphogenesis of Kidney Cortical Peritubular Capillaries in Angiopoietin-2-Deficient Mice

Jolanta E. Pitera,* Adrian S. Woolf,* Nicholas W. Gale,† George D. Yancopoulos,† and Hai Tao Yuan*‡

From the Institute of Child Health, University College London, London, United Kingdom; Regeneron Pharmaceuticals Inc,† Tarrytown, New York; and Harvard Medical School,‡ Renal Division, Department of Medicine, Beth Israel Deaconess Medical Center, Boston, Massachusetts*

Angiopoietin-2 (Ang-2) modulates Tie-2 receptor activation. In mouse kidney maturation, Ang-2 is expressed in arteries, with lower levels in tubules, whereas Tie-2 is expressed by endothelia. We hypothesized that Ang-2 deficiency disrupts kidney vessel patterning. The normal renal cortical peritubular space contains fenestrated capillaries, which have few pericytes; they receive water and solutes which proximal tubules reclaim from the glomerular filtrate. In wild-type neonates, α smooth muscle actin (αSMA), platelet-derived growth factor receptor β (PDGFRβ), and desmin-expressing cells were not prominent in this compartment. In *Ang-2* null mutants, αSMA, desmin, and PDGFRβ prominently immunolocalized in cortical peritubular locations. Some αSMA-positive cells were closely associated with CD31- and Tie-2-positive peritubular capillary endothelia, and some of the αSMA-positive cells expressed PDGFRβ, desmin, and neural/glial cell 2 (NG2), consistent with a pericyte-like identity. Immunoblotting suggested an increase of total and tyrosine-phosphorylated Tie-2 proteins in null mutant versus wild-type kidneys, and electron microscopy confirmed disorganized capillaries and adjacent cells in cortical peritubular spaces in mutant neonate kidneys. Hence, Ang-2 deficiency causes dysmorphogenesis of cortical peritubular capillaries, with adjacent cells expressing pericyte-like markers; we speculate the latter effect is caused by disturbed paracrine signaling between endothelial and surrounding mesenchymal precursor cells. ***(Am J Pathol 2004, 165:1895–1906)***

In adult mammals, 20% of the cardiac output flows through the kidneys. At embryonic day 11 (E11), the mouse metanephros, the adult kidney precursor, forms when renal mesenchyme condenses around the ureteric bud.[1] This rudiment contains no formed vessels, although metanephric mesenchyme expresses vascular endothelial growth factor receptors (VEGFR), and transplantation experiments suggest that it harbors endothelial cell (EC) precursors.[2–6] By E13, capillaries form networks around epithelial tubules; these vessels express EC markers including CD31 and VEGFR. At E14, the rudiment contains a single hilar artery and first-order (interlobar) renal artery (RA) branches which later form corticomedullary junction "arcades."[1,7] Cortical (interlobular) arteries branch from arcades and they themselves branch, forming afferent glomerular arterioles. From E14, α smooth muscle actin (αSMA) is expressed in vascular smooth muscle cells (VSMC) of larger RA[7] and, from E15, the first layer of glomeruli acquires capillary loops supported by mesangial pericytes. At birth, the mouse kidney contains around 1500 glomeruli but the rest form in the next week, resulting in 10^4 nephrons.[7]

Apart from glomerular capillaries, the kidney contains other blood capillary networks: 1) one occupies the spaces between cortical, predominantly proximal, tubules, and it arises from the efferent arteries of superficial glomeruli; these fenestrated capillaries have few, if any, pericytes[8] and hence are able to receive with minimal structural impediment water and solutes which have been reclaimed from the glomerular filtrate by adjacent tubules; 2) another capillary network, the vasa rectae, arises from efferent arterioles of deep glomeruli; these descend into the medulla as pericyte-coated vessels and, together with fenestrated ascending vasa rectae, are involved in urinary concentration. In mice, renal capillaries surrounding proximal tubules in the cortex be-

Supported by the Kidney Research Aid Fund (H.T.Y.) and the National Kidney Research Fund project grant R4/2/2001 (to J.E.P.). G.D.Y. and N.W.G. are affiliated with Regeneron Pharmaceuticals Inc., Tarrytown, NY, USA.

Accepted for publication August 16, 2004.

Address reprint requests to Dr. Hai Tao Yuan, Harvard Medical School, Renal Division, Department of Medicine, Beth Israel Deaconess Medical Center, 330 Brookline Avenue, Dana 517, Boston, MA 02115. E-mail: hyuan@bidmc.harvard.edu.

come prominent from the late fetal period whereas vasa rectae mature 1 to 3 weeks postnatally.[1]

Genetic and pharmacological strategies have proven that VEGF-A is important in glomerular capillary growth,[9,10] and transgenic expression of EphB4 receptor, a gene expressed in developing kidney vessels,[11] perturbs glomerular arteriole patterning.[12] Mutant mice have implicated platelet-derived growth factor B (PDGFB) signaling in mesangial morphogenesis[13,14] and also α8 integrin in morphogenesis of peritubular capillaries.[15] Other molecules including transforming growth factor β1 and fibroblast growth factor 2 may facilitate renal vessel growth.[16,17] However, little is understood about molecules which might control the normal maturation of non-glomerular capillary beds.

Angiopoietins are a family of growth factors binding to Tie-2, a receptor tyrosine kinase.[18–22] Angiopoietin-1 (Ang-1) causes endothelial cell (EC) Tie-2 tyrosine autophosphorylation, with context-dependent effects including EC survival, and capillary stabilization and sprouting.[23,24] *Ang-1* null mutant mice have defective endocardial differentiation and, in other locations, primary vascular networks fail to remodel normally; additionally, supporting cells such as cardiomyocytes and pericytes/VSMC form incompletely, probably due to secondary disruption of signaling between EC and adjacent mesenchymal precursors. VSMC begin differentiation as "fibroblast-like" cells, lacking myofilaments and basement membranes and appearing as aggregates near embryonic EC.[25] Cell lineage studies in birds suggest that aortic arch VSMC are derived from ectoderm (ie, neural crest), whereas VSMC in other sites are mesodermally derived. However, there is also evidence that embryonic avian dorsal aortic EC transdifferentiate into myofilament-expressing mesenchymal cells.[26] Pericytes, the cells which surround EC in many capillary beds, are related to VSMC but their biology is complex. As examples: 1) pericytes cover different capillary beds to greatly differing extents, eg, EC involved in transport of nutrients and/or gases such as renal cortical peritubular capillaries, are pericyte-free;[8] 2) the proteins that pericytes express vary depending on their location, their state differentiation, and whether they are involved in normal developing or adult, or pathological, vasculature, eg, in terms of αSMA, desmin, the neural/glial cell 2 (NG2) chondroitin sulfate proteoglycan, and PDGFRβ expression;[27,28] and 3) pericytes themselves can differentiate into VSMC, fibroblasts, and other mesenchymal-derived cell types such as osteoblasts.[29] In addition, the ontogeny of pericytes is poorly understood, although paracrine signaling via EC-derived PDGFB is important, with this growth factor directing the growth and migration of mesenchymal cells which themselves express PDGFRβ.[30,31]

Transgenic Ang-2 overexpression produces defects resembling *Ang-1* null mutants and initial work demonstrated that Ang-2 bound to, but did not activate, EC Tie-2;[32] hence, Ang-2 was considered an Ang-1 inhibitor. More recently, other Ang-2 actions were discovered. In certain settings, Ang-2 triggers EC Tie-2 phosphorylation, enhancing vessel growth;[33–35] second, *Ang-2* null mutant mice have disordered lymphatics because Ang-2 stimulates lymphatic capillary maturation;[20] and third, Ang-2 can support EC adhesion independently from Tie-2 signaling.[36] Ang-2 modulates remodeling of ocular blood capillaries[20,37] but its possible functions in differentiation of other organs is unknown. Tie-2, and its Ang-1 and Ang-2 ligands, are expressed in the mouse metanephros and in the mature organ, with total levels peaking in perinatally.[5,7,38–40] In the late fetal period, Ang-1 is expressed by glomerular epithelia and diverse tubules, whereas Ang-2 is expressed by renal arterial walls, with lower levels in tubules. Tie-2 is expressed by differentiating renal EC. Based on known expression patterns of Ang-2 and Tie-2 genes, We hypothesized that lack of Ang-2 disrupts kidney vessel patterning. We therefore assessed kidneys from *Ang-2* mutant mice. In this study, we demonstrate that Ang-2 is most likely implicated in the differentiation of a non-glomerular renal microcirculation, namely the cortical peritubular capillaries and associated cells.

Materials and Methods

Reagents and Animals

Reagents were obtained from Sigma Chemical Company (Poole, UK), unless otherwise stated. Primary antibodies used were αSMA alone or conjugated (clone 1A4), αSMA conjugated with horseradish peroxidase (HRP) (U7033; DAKO, High Wycombe, UK), CD31 (BD Biosciences, San Diego, CA), F4/80 macrophage marker (Serotec, Oxford, UK), phosphotyrosine (PY-99; Santa Cruz Biotechnology Inc, Santa Cruz, CA), desmin (D33; DAKO), NG2 proteoglycan (Chemicon, Hampshire, UK), PDGFRβ (BD Biosciences, Oxford, UK), Tie-2 (Santa Cruz), and Tie-2 (a gift from Toshio Suda, Kumamoto University School of Medicine, Japan). Animal experiments were performed with UK Home Office permission. Mice heterozygous for an *Ang-2* inactivating mutation, with *LacZ* encoding β-galactosidase substituted as a reporter gene for normal Ang-2 expression, were provided by Regeneron Pharmaceuticals, Inc (Tarrytown, NY).[7,20] We refer to wild-type mice as *Ang-2*$^{+/+}$, heterozygous animals as *Ang-2*$^{+/LZ}$, and null mutant mice as *Ang-2*$^{LZ/LZ}$. Mice were genotyped as described.[7] *Ang-2*$^{+/LZ}$ mice were maintained by mating with 129SV mice (Charles River Ltd, UK) for more than 10 generations, so this study describes the mutation effectively on a 129SV background. *Ang-2*$^{+/LZ}$ parents were mated to generate *Ang-2*$^{+/+}$, *Ang-2*$^{+/LZ}$, and *Ang-2*$^{LZ/LZ}$ progeny. In preliminary experiments, *Ang-2*$^{LZ/LZ}$ mice appeared healthy on the first day of life (P1). By P3, all *Ang-2*$^{LZ/LZ}$ mice had chylous ascites, as described,[20] and they died by 1 week of age. We therefore studied E14, E17, and P1 litters.

Whole Mount Staining

Kidneys were visualized with the X-gal (4-chloro-5-bromo-3-indolyl-β-D-galactopyranoside) reaction as described,[3,4,7] allowing optimal detection of cytoplasmic reporter *LacZ* gene product, while abolishing back-

ground staining. Ang-2 is expressed by RA[7,39] and preliminary studies revealed that first-order RA branches could be visualized after the X-gal reaction in *Ang-2*$^{+/LZ}$ and *Ang-2*$^{LZ/LZ}$ organs. Their number (per two E17 kidneys in each animal) was quantified by summating branches on anterior and posterior faces of whole mounts. For *LacZ* expression, we examined 63 animals at E17, with a minimum of 9 animals of each genotype, and 18 at P1, with a minimum of 4 animals of each genotype. For immunostaining, the protocol of Pitera et al[41] was used; primary antibodies (αSMA, 1:1000; CD31, 1:1000; PDGFRβ, 1:500; and Tie2, 1:1000) were applied, organs incubated with HRP-conjugated secondary antibodies and signals generated with DAB. For these whole mount immunostaining studies we examined 6 animals at E14 (using αSMA antibody), 26 at E17, and 34 at P1 (using all antibodies), with approximate distributions of 1:1:1 for the three genotypes.

Electron Microscopy and Bright Field Immunohistochemistry

Other sets of kidneys were processed for electron microscopy (EM) and bright field microscopy as described.[3,7] In the latter cases, some sections were processed for immunostaining after pretreatment to optimize antigen retrieval using pronase (DAKO) and/or heat treatment using Retrievagen buffer (BD Biosciences, CA). Endogenous peroxidase was quenched with 3% H_2O_2 for 30 minutes, sections were blocked with 20% heat-inactivated fetal calf serum, 0.2% bovine serum albumin (BSA) and 0.1% Tween-20 in phosphate-buffered saline (PBS), and were incubated overnight with antibodies (αSMA-conjugated HRP, 1:1; CD31, 1:1000; desmin, 1:500; Tie-2, 1:500; and F4/80, 1:4000). Cortical capillary area was quantified by CD31 immunostaining, as described.[42] Positive signal was captured using the Magic Wand Tool of Adobe Photoshop 5.5.

Double-Immunofluorescence Studies

For desmin/αSMA and PDGFRβ/αSMA double-immunofluorescence studies, the following protocol was used: P1 kidneys were fixed for 20 minutes in 4% paraformaldehyde and 8-μm frozen sections were cut; sections were then blocked at room temperature with 20% fetal calf serum (FCS) and 2% bovine serum albumin (BSA); desmin (1:200) or PDGFRβ (1:600) antibodies were applied for 1 hour at room temperature and appropriate second antibodies conjugated to Alexa Fluor 488 (Molecular Probes, Leiden, Netherlands) were then applied. For CD31/αSMA, Tie-2/αSMA, and NG2/αSMA double-immunofluorescence studies, the following protocol was used: 8-μm frozen sections were cut from unfixed P1 kidneys; sections were fixed for 10 minutes in ice-cold acetone and blocked for 15 minutes at room temperature with 20% fetal calf serum, 0.1% Tween 20, and 2% bovine serum albumin; CD31 (1:000), Tie-2 (1:300), or NG2 (1:50) antibodies were applied for 1 hour at room temperature and appropriate second antibodies conjugated to Alexa Fluor 488 were then applied. All protocols were finished as follows; after several washes in PBS, Cy3-conjugated anti-αSMA (1:500) was applied and sections covered in anti-fading fluorescence mountant (DAKO). Color images were obtained with Leica confocal microscope with windows set for appropriate emission wavelengths (eg, 519 nm for Alexa Fluor 488 and 570 nm for Cy3). Alexa Fluor 488 signal appears green while the Cy3 signal appears red, with co-expression appearing as a yellow color. To save space, representative pictures from the double-immunofluorescence studies are depicted in the Results section as merged images only. Preliminary experiments demonstrated that there was no overlap between the two windows (data not shown); furthermore, using these conditions, no significant signal was observed in any experiments when primary antibodies were omitted (data not shown).

Northern and Western Blotting and Immunoprecipitation for Phosphorylated Tie-2

Northern blot was performed as described.[38] Twenty μg of total RNA from pools of six P1 kidneys from each genotype was hybridized using mouse Ang-1 and Ang-2 probes. Mouse 18S rRNA cDNA was used to factor for sample loading. Western blotting was performed as described.[38] For αSMA, 60 μg of protein samples from pools of 10 P1 kidneys from each genotype was separated on 6 to 12% SDS-PAGE gels. For detection of total and phosphorylated Tie-2 protein, 1 mg of protein (which required around 30 kidneys from each genotype) was immunoprecipitated with Tie-2 antibody and Protein-A agarose (Santa Cruz). Primary antibodies used to probe blots were αSMA, 1:10,000; Tie-2, 1:1000; anti-phosphotyrosine, 1:500, and HRP-conjugated second antibodies, 1:1500. Western blots for αSMA were stripped and reprobed with antibody to GAPDH (1:1000), a "housekeeping" protein. Bands were measured by densitometry. αSMA/GAPDH results were expressed as mean ± SD and were compared by unpaired Student's *t*-test. For total and phosphorylated Tie-2, only two experiments were performed due to the large amounts of protein/organs needed for the assays and data from the two separate experiments are shown in the Results section.

Statistics

Parameters were expressed as mean ± SD and groups compared using unpaired Student's *t*-test or by one-way analysis of variance followed by *t*-tests.

Results

Northern Blot

An Ang-2 transcript was detected in *Ang-2*$^{+/+}$ P1 kidneys, with a fainter band in heterozygous, and no signal in *Ang-2*$^{LZ/LZ}$ organs (Figure 1). Ang-1 transcript was

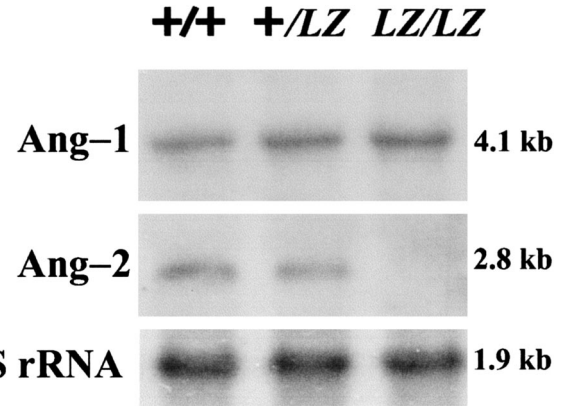

Figure 1. Northern blot of P1 kidneys. Northern blot, representative of two experiments, for Ang-1, Ang-2, and 18S rRNA in pools of P1 kidneys. Ang-2 signal was absent in the *Ang-2$^{LZ/LZ}$* organs, whereas Ang-1 and 18S rNRA was detected in this genotype.

detected in all genotypes. Hence *Ang-2$^{LZ/LZ}$* was a true null mutation and was specific for Ang-2 versus Ang-1.

Overview of Growth

At E14, E17, and P1, for all genotypes, each animal examined had two kidneys and no anomalies of the lower urinary tract (dilatation, obstructive lesions, or bladder malformation) were detected. No ascites was observed at laparotomy on E14 and E17. Expected Mendelian ratios were observed for P1 offspring of *Ang-2$^{+/LZ}$* parents; of 178 from 21 litters, 48 were *Ang-2$^{+/+}$*, 86 were *Ang-2$^{+/LZ}$* and 44 were *Ang-2$^{LZ/LZ}$*. All P1 *Ang-2$^{LZ/LZ}$* mice appeared healthy eg, in activity and external appearance, but 10 had free chyle on laparotomy. There was no significant difference of P1 body weights between the three genotypes, although *Ang-2$^{LZ/LZ}$* mice had modest but significantly reduced kidney and kidney/body weights versus *Ang-2$^{+/LZ}$* and *Ang-2$^{+/+}$* mice (Table 1).

LacZ Expression

E17 *Ang-2$^{+/+}$* organs were negative after the X-gal reaction (Figure 2A). LacZ expressing RA were observed in E17 *Ang-2$^{+/LZ}$* and *Ang-2$^{LZ/LZ}$* whole mounts (Figure 2, B and C). There was no significant difference in absolute numbers of first-order RA branches between the genotypes, although there was a marginally significant (P = 0.05) decrease in the number of first-order branches in

Table 1. Body and Kidney Weights of *P1* Mice

	Body weight (g)	Single kidney weight (mg)	Kidney/body weight (%)
Ang-2$^{+/+}$ (n = 16)	1.57 ± 0.18	7.5 ± 0.7	0.48 ± 0.06
Ang-2$^{+/LZ}$ (n = 30)	1.59 ± 0.13	7.4 ± 0.9	0.47 ± 0.06
Ang-2$^{LZ/LZ}$ (n = 17)	1.48 ± 0.20	6.1 ± 0.8*	0.42 ± 0.07†

Measurements are mean ± SD. All animals from six litters were examined. *$P < 0.01$ versus *Ang-2$^{+/+}$* and *Ang-2$^{+/LZ}$*, †$P < 0.05$ versus *Ang-2$^{+/+}$* and *Ang-2$^{+/LZ}$*.

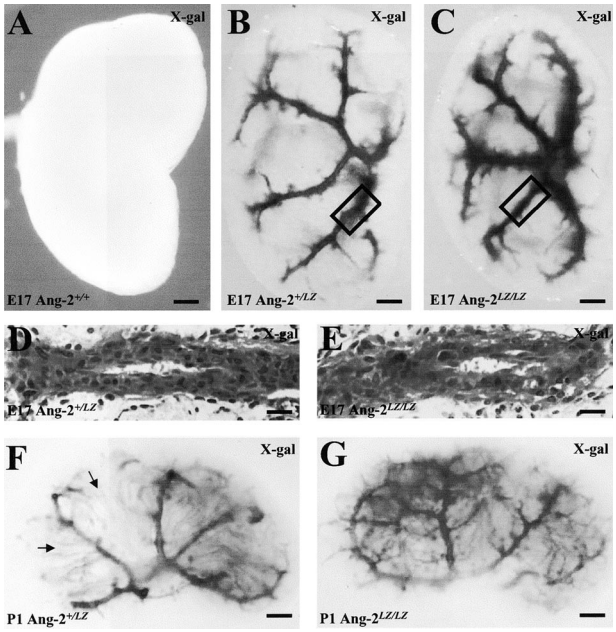

Figure 2. LacZ expression. Whole mounts of *Ang-2$^{+/+}$* (**A**), *Ang-2$^{+/LZ}$* (**B**) and *Ang-2$^{LZ/LZ}$* (**C**) littermate E17 metanephric kidneys; X-gal reaction produces a black signal. Representative pictures are shown from kidneys from 9 to 17 embryos from each genotype. Boxes in B and C indicate first-order RA branches depicted in sections from *Ang-2$^{+/LZ}$* (**D**) and *Ang-2$^{LZ/LZ}$* (**E**) kidneys; note that **D** and **E** sections are counterstained with hematoxylin. P1 *Ang-2$^{+/LZ}$* (**F**) and *Ang-2$^{LZ/LZ}$* (**G**) P1 kidneys from one litter; no staining was observed in *Ang-2$^{+/+}$* organs (not shown). Representative pictures are shown from four organs of each genotype. The impression of more prominent arteries visualized in *Ang-2$^{LZ/LZ}$* whole mounts (eg, **C** versus **B**) is probably explained by the fact that homozygous mice have "two doses" of the *LacZ* transgene whereas heterozygous mice have only one *LacZ* allele. **Arrows** in **F** indicate LacZ-expressing tubules. **Bars:** 500 μm, **A** to **C**; 30 μm, **D** and **E;** 1000 μm, **F** and **G**.

Ang-2$^{LZ/LZ}$ kidneys when factored for body weight (Table 2) because the average body weights of null mutants were marginally higher than those of heterozygous animals. We cannot rule out the possibility, however, that the body weights of *Ang-2$^{LZ/LZ}$* animals were "artificially elevated" by a degree of subclinical edema. On the other hand, E17 *Ang-2$^{LZ/LZ}$* fetuses did not have peripheral edema or ascites detectable by the naked eye. Histologically, no major structural differences in RA were discerned between genotypes (Figure 2, D and E). At P1, the pattern of LacZ-expressing vessels in mutant genotypes was more complex and could not be quantified as for E17 organs; however, no major differences were noted between *Ang-2$^{+/LZ}$* and *Ang-2$^{LZ/LZ}$* kidneys (Figure 2, F and G). LacZ was also expressed in radially ar-

Table 2. E17 RA Branches Assessed by X-gal

	Numbers of branches	Body weight (g)	Branches/body weight
Ang-2$^{+/LZ}$ (n = 9)	17.7 ± 1.7	0.89 ± 0.20	20.4 ± 3.6
Ang-2$^{LZ/LZ}$ (n = 17)	16.1 ± 2.0	0.96 ± 0.18	16.1 ± 1.9*

"Numbers of branches" indicate the total number of main first-order RA branches in both kidneys from one animal. Measurements are mean ± SD. Embryonic kidneys were chosen randomly from several sets of litters. *P = 0.05 versus *Ang-2$^{+/+}$*.

ranged structures (eg, arrows in Figure 2F), which are terminal portions of proximal tubules and thin descending limbs of loops of Henle.[7,38]

αSMA Expression

The first Ang-2 expressing RA appear at E14.[7] At this stage, there was no discernable difference in whole mount αSMA expression, with immunoreactivity only detected in large RA (two to three embryos examined from each genotype; data not shown). In *Ang-2*$^{+/+}$ E17 kidneys, a pattern of first-order RA branches was detected similar to the LacZ expression pattern described above (compare Figure 3A with 2B). In *Ang-2*$^{+/LZ}$ E17 kidneys, a similar pattern was noted (Figure 3B), whereas this pattern was not evident in *Ang-2*$^{LZ/LZ}$ littermates (Figure 3C), even though *Ang-2*$^{LZ/LZ}$ organs had a grossly normal pattern of major RA as assessed by LacZ expression (see Figure 2, C and E), and first-order RA were also detected by αSMA immunohistochemistry (not shown). Instead, when *Ang-2*$^{LZ/LZ}$ whole mounts were viewed *en face*, a reticular aSMA pattern was evident (Figure 3C). Similar observations were made in P1 kidneys (Figure 3, D and E, and data not shown). In the cortex of *Ang-2*$^{+/+}$ P1 kidneys (Figure 3F), αSMA immunostaining was detected in small arteries and arterioles but signal was absent in the interstitial spaces between proximal and other tubules just below the nephrogenic zone. In *Ang-2*$^{LZ/LZ}$ kidneys (Figure 3G), prominent αSMA signals were detected between proximal and other tubules immediately below the nephrogenic zone, apparently correlating with the altered αSMA immunostaining visualized in whole mounts of mutant mice (Figure 3E). Glomeruli were detected in both *Ang-2*$^{+/+}$ and *Ang-2*$^{LZ/LZ}$ organs, with no gross difference on histology. The impression of increased αSMA in *Ang-2*$^{LZ/LZ}$ versus wild-type littermate P1 kidneys was confirmed both by Western blot and densitometry (Figure 3, H and I).

Electron Microscopy

In toluidine blue-stained ultra-thin sections of P1 kidneys, intertubular spaces in the cortex of *Ang-2*$^{LZ/LZ}$ mice were noted to be disorganized versus wild-type littermate kidneys (Figure 4, A and B). On EM, in *Ang-2*$^{+/+}$ kidneys, peritubular capillaries were typically comprised of single lines of vessels (Figure 4C). In the *Ang-2*$^{LZ/LZ}$ kidney, however, these spaces were occupied by structures with multiple lumens with prominent, often loosely approximating, interstitial cells (Figure 4D). The former may represent dysmorphogenic capillaries, whereas the latter may be αSMA ± NG2/PDGFRβ/desmin-expressing cells described below. Although the peritubular spaces appeared abnormal as assessed by EM, the cortical capillary area, quantified by CD31 immunostaining, as described in Materials and Methods, was not different between wild-type and null mutant kidneys (mean of 25% and 23%, respectively). Macrophages are a known cell type in the renal interstitium but immunostaining with F4/80 revealed only sparse positive cells in *Ang-2*$^{+/+}$ and *Ang-2*$^{LZ/LZ}$ renal cortex (data not shown). Other EM data (not shown) showed glomeruli with podocytes, capillary loops, and mesangial cells in both *Ang-2*$^{+/+}$ and *Ang-2*$^{LZ/LZ}$ kidneys.

Tie-2 Expression

In whole mounts immunostained for Tie-2, E17, and P1 *Ang-2*$^{+/+}$ kidneys displayed a reticular pattern which appeared more prominent in *Ang-2*$^{LZ/LZ}$ organs (Figure 5, A and B; and data not shown). Using histochemistry, apparently more prominent Tie-2 immunostaining was detected in P1 peritubular capillaries in *Ang-2*$^{LZ/LZ}$ versus *Ang-2*$^{+/+}$ organs (Figure 5, C and D). In P1 kidneys, immunoblot and densitometry detected a more prominent band for both phosphorylated Tie-2 and total Tie-2 in *Ang-2*$^{LZ/LZ}$ versus *Ang-2*$^{+/+}$ littermate kidneys (Figure 5, E and F). For these biochemical assays, only two sets of experiments could be performed, due to the large amounts of protein (1 mg, representing several tens of organs) needed for each individual assay.

Double-Immunofluorescence Studies

To clarify the relationship between endothelial and pericyte markers, we performed a series of double-immunofluorescence experiments on sections of P1 *Ang-2*$^{+/+}$ versus *Ang-2*$^{LZ/LZ}$ littermate kidneys in which αSMA was detected with Cy3, producing a red signal, and other proteins were detected with Alexa Fluor 488, producing a green signal (Figure 6, A to H). To save space, representative pictures from the double-immunofluorescence studies from four to five animals of each genotype are depicted as merged images only; in these frames, cells that co-express the two proteins under study would appear yellow. In wild-type organs, networks of CD31- (Figure 6A) and Tie-2- (Figure 6E) expressing capillaries were noted in the nephrogenic zone and between cortical tubules underneath this zone; in these fields, significant αSMA signal was only noted in the walls of arterial vessels. High-power views of *Ang-2*$^{+/+}$ peritubular capillaries confirmed that they were not associated with αSMA-expressing cells (Figure 6, C and G). Low-power views of the kidney cortex of null mutant kidneys revealed prominent αSMA expression in a reticular pattern around tubules (Figure 6, B and F) and high-power views made it clear that CD31- and Tie-2-positive endothelia of peritubular capillaries were often surrounded by a population of cells expressing αSMA (Figure 6, D and H). By scanning through these sections, we also noted that αSMA signal did not cover the surface of every capillary, and not all αSMA-expressing cells in the peritubular compartment were closely associated with endothelia. Cells expressing both an endothelial marker and also αSMA were not seen in the null mutants (note that, in some high-power views, tiny yellow "speckles" are seen at the interface between EC and adjacent cells, which most likely represent interdigitations between these cells which overlap in the same confocal section).

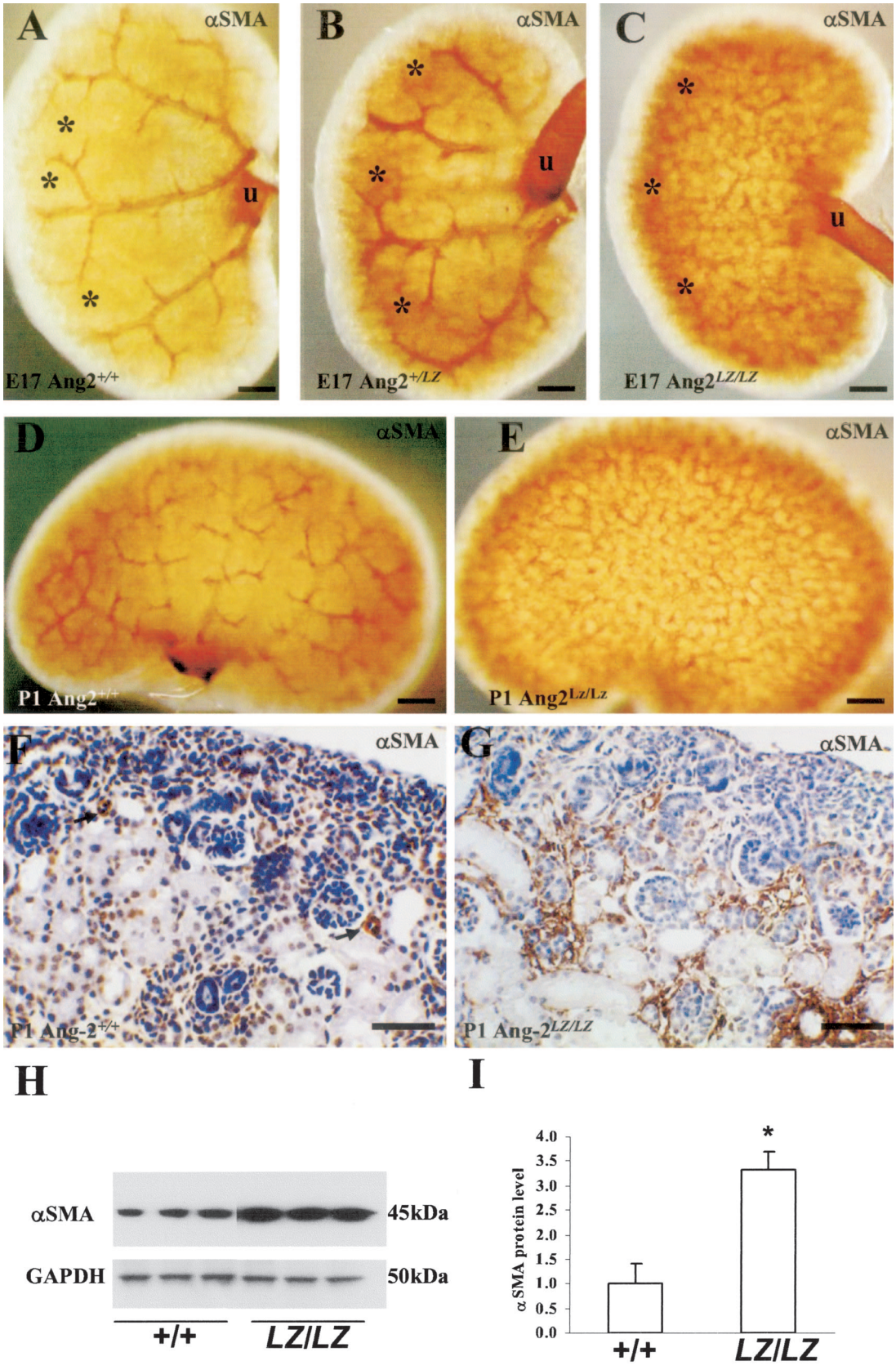
A
αSMA
u
E17 Ang2+/+
B
αSMA
u
E17 Ang2+/LZ
C
αSMA
u
E17 Ang2LZ/LZ
D
αSMA
P1 Ang2+/+
E
αSMA
P1 Ang2Lz/Lz
F
αSMA
P1 Ang-2+/+
G
αSMA
P1 Ang-2LZ/LZ
H
αSMA
45kDa
GAPDH
50kDa
+/+
LZ/LZ
I
αSMA protein level
4.0
3.5
3.0
2.5
2.0
1.5
1.0
0.5
0.0
*
+/+
LZ/LZ

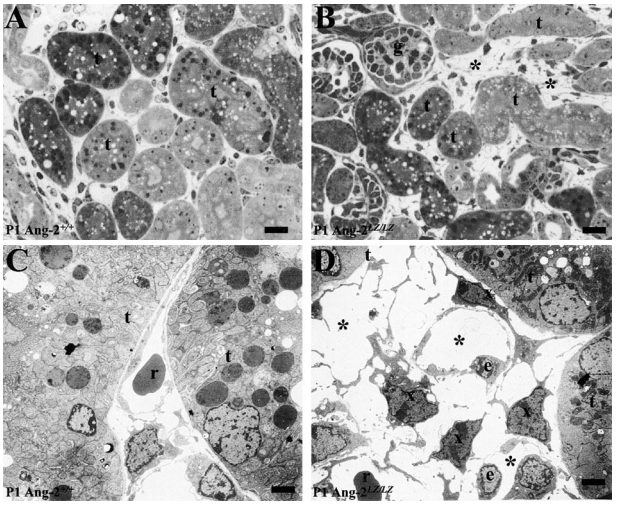

Figure 4. Cortical peritubular spaces. **A** and **B** were toluidine blue-stained ultra-thin sections, and **C** and **D** are EM. **A** and **C** are *Ang-2*$^{+/+}$ kidneys and **B** and **D** were *Ang-2*$^{LZ/LZ}$ littermates. Note apparently disorganized peritubular spaces in the mutant organ (**asterisk** in **B**) versus *Ang-2*$^{+/+}$ organ (**A**). Tubules (t) and a glomerulus (g) are indicted. In an *Ang-2*$^{+/+}$ kidney (**C**), a single capillary containing a red cell (r) occupied the space between tubules (t), whereas, in the *Ang-2*$^{LZ/LZ}$ kidney (**D**), the space was occupied by multiple lumens (*), some containing red cells. Prominent, polygonal, or elongated dark cells (x) were located near EC bodies (e) in the *Ang-2*$^{LZ/LZ}$ kidney. **Bars**: 15 μm, **A** and **B**; 2.5 μm, **C** and **D**.

Next, we performed further double-immunofluorescence studies to attempt to ascertain whether peritubular αSMA cells in *Ang-2*$^{LZ/LZ}$ kidneys might also express other "pericyte markers", namely NG2, PDGFRβ, and desmin (Figure 7, A to L). In wild-type organs: 1) NG2 was immunolocalized to the outer layers of arterial vessels (Figure 7A) and also to cells in peritubular spaces (Figure 7, A and C); 2) a faint PDGFRβ signal was detected in some glomeruli and peritubular regions in the deeper cortex (Figure 7E and data not shown) but no significant signal was found near to peritubular capillaries (Figure 7G); and 3) a faint desmin signal was detected in the nephrogenic zone (Figure 7I). Low-power views of the cortex of null mutant mice revealed a striking increase of expression of NG2 (Figure 7B), PDGFRβ (Figure 7F), and desmin (Figure 7J). Detailed views of the cortical peritubular spaces of *Ang-2*$^{LZ/LZ}$ kidneys showed that some, but not all, of the cells positive for αSMA also expressed NG2 (Figure 7D), PDGFRβ (Figure 7H), and desmin (Figure 7L) proteins. Although these sections were not probed with capillary markers, many of the co-expressing cells appeared to surround "lumens", some of which may have represented peritubular capillary spaces.

Discussion

Ang-2 actions *in vivo* are thought to depend on levels of VEGF; when ambient VEGF is low, Ang-2 causes vessel regression (eg, involuting corpus luteum), whereas Ang-2 destabilizes vessels and facilitate sprouting with plentiful VEGF (eg, tumors).[21,43] It is established that the developing kidney expresses VEGF[3,9] and, additionally, Ang-1 and Ang-2 mRNA levels in mice peak around the neonatal period.[38] Removal or reduction of the influence of Ang-2, as achieved in this study by genetic ablation, would allow VEGF and Ang-1 actions to continue without a modulating, possibly inhibitory, effect of Ang-2. Our data showed dysmorphogenesis of the cortical peritubular capillaries especially with regard to associated pericyte-like cells. In addition, we found a trend toward an increase of total and probably also phosphorylated Tie-2 protein, when assessed by immunoblotting of neonatal kidneys. Further experiments will be necessary, however, using cell biology and biochemical techniques, to unravel whether the genetic deletion of Ang-2 may have led to either an activation or inhibition of Tie-2 activity at the level of individual renal EC. Collectively, the data presented in the current study show that Ang-2 deficiency is associated with aberrant differentiation of cells surrounding renal cortical peritubular capillaries and we speculate that this is caused by enhanced paracrine signaling between endothelia and surrounding mesenchymal precursor cells.

Recently, Ang-2 has been implicated in lymphatic growth;[20] indeed, *Ang-2* null mutant mice develop chylous ascites and most probably die directly because of this pathology. Furthermore, both dermal blood and lymphatic capillaries express Tie-2 in culture.[44] A question therefore arises whether the disordered kidney peritubular vessels we observed might be lymphatic, rather than blood, capillaries. We think this is unlikely for three reasons. First, in mature kidneys, lymphatics are associated with RA, reaching glomeruli along afferent arterioles, but they are not found in the peritubular cortical spaces.[45] Second, in *Ang-2*$^{LZ/LZ}$ kidneys, red blood cells were often observed on EM in dysmorphic peritubular vessels. Third, our unpublished data shows that the peritubular regions of *Ang-2*$^{LZ/LZ}$ kidneys do not show abnormal immunostaining for Prox-1, a transcription factor expressed by developing lymphatic capillaries.[46]

The most striking positive finding in this study was that αSMA-expressing cells were up-regulated in renal cortical peritubular locations in mutant mice. A trivial explanation for this finding might be that the null mutant kidney

Figure 3. Whole mount αSMA immunostaining. Ang-2$^{+/+}$ (**A**), *Ang-2*$^{+/LZ}$ (**B**) and *Ang-2*$^{LZ/LZ}$ (**C**) littermate E17 kidneys; representative views are shown from organs of three to five embryos for each genotype. The ureter (u) expresses αSMA (brown) in its muscle layer. The pattern of major RA was progressively obscured in *Ang-2*$^{+/LZ}$ (**B**) and *Ang-2*$^{LZ/LZ}$ (**C**) metanephroi. A cortical zone (* in **A**, **B**, and **C**) immunostained progressively more intensely for αSMA in heterozygous and *Ang-2*$^{LZ/LZ}$ kidneys. Whole mounts of *Ang-2*$^{+/+}$ (**D**) and *Ang-2*$^{LZ/LZ}$ (**E**) P1 littermate kidneys; representative views are shown from organs of three to four animals for each genotype. Again, the pattern of major RA was obscured in *Ang-2*$^{LZ/LZ}$ organs by a reticular pattern of αSMA-positive structures. **F** and **G:** Sections of P1 *Ang-2*$^{+/+}$ and *Ang-2*$^{LZ/LZ}$ littermate organs; views are representative of kidney cortex from six animals of each genotype. Sections were immunostained for αSMA (brown) and counterstained with hematoxylin. αSMA signal was evident in small arteries (**arrows**) in wild-type kidneys, whereas αSMA immunostaining was prominent between tubules in *Ang-2*$^{LZ/LZ}$ kidneys. **H:** Western blot of three separate pools of 10 P1 kidneys of wild-type and null mutant genotype; note apparently increased αSMA (45 kd) in *Ang-2*$^{LZ/LZ}$ organs, with similar levels of GAPDH (50 kd). **I:** Densitometry of αSMA bands shown in **H**, factored for GAPDH; **bars** show mean ± SD (n = three pools of kidneys), and the **asterisk** indicates $P < 0.01$ *Ang-2*$^{LZ/LZ}$ organs versus wild-type. **Bars**: 500 μm, **A** to **C**; 1000 μm, **D** and **E**; 60 μm, **F** and **G**.

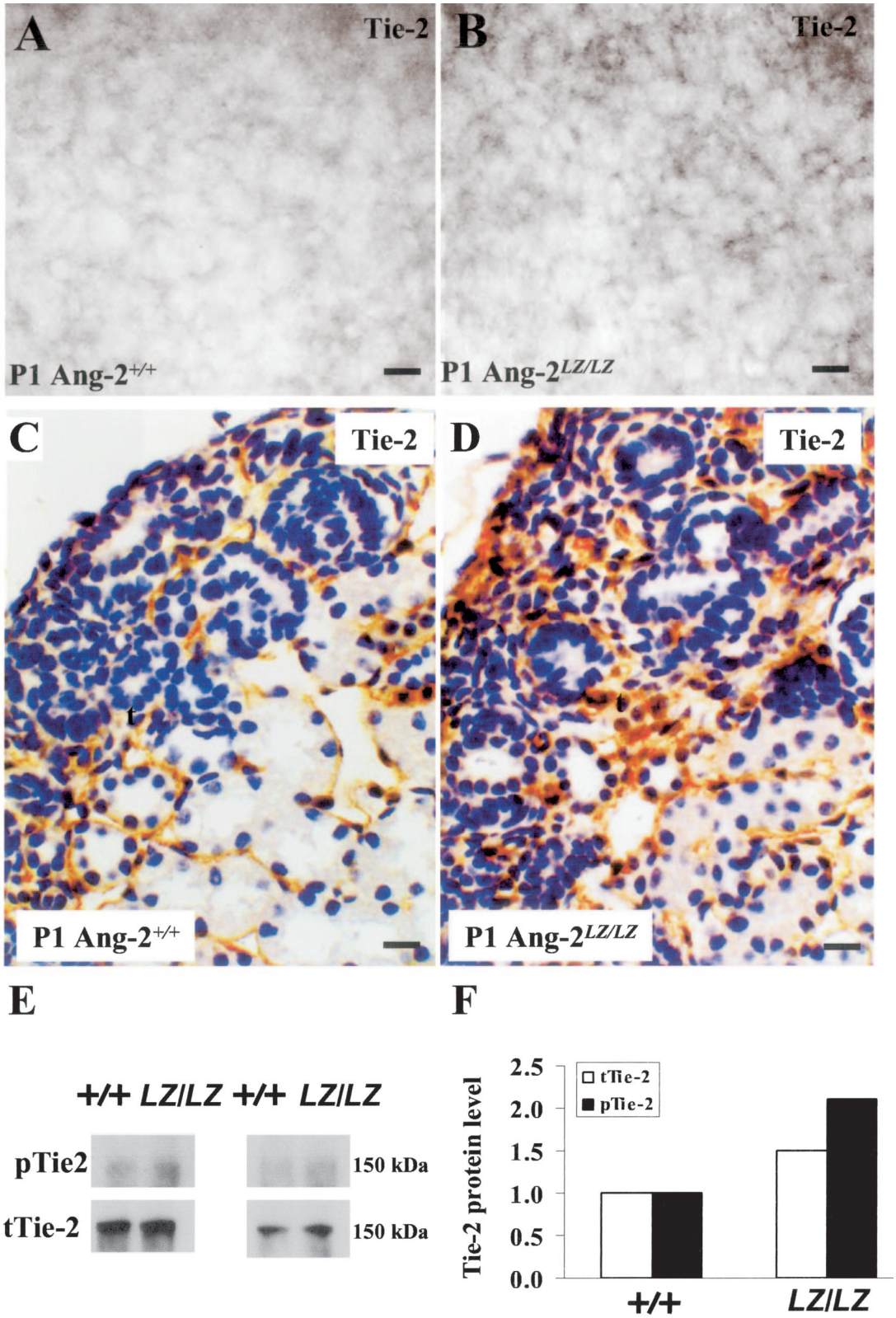

Figure 5. Tie-2 expression. Whole mounts of *Ang-2*$^{+/+}$ (**A**) and *Ang-2*$^{LZ/LZ}$ (**B**) littermate P1 kidneys immunostained for Tie-2; representative views are shown from organs of three animals for each genotype. Note the apparently increased signal (**gray** in these black and white photos) in the *Ang-2*$^{LZ/LZ}$ organs. **C** and **D**, respectively, show Tie-2 immunohistochemistry P1 *Ang-2*$^{+/+}$ and *Ang-2*$^{LZ/LZ}$ P1 kidneys; note Tie-2 immunostaining between tubules in *Ang-2*$^{+/+}$ and in *Ang-2*$^{LZ/LZ}$ kidney. **E:** Immunoprecipitation of Tie-2 protein from P1 kidney pools. Phosphorylated Tie-2 (*p-Tie-2*) and total Tie-2 (*t-Tie-2*) were respectively detected using anti-phosphorylated tyrosine antibody and Tie-2 antibody. Results show two representative experiments using different sets of starting material, with each **lane** run with equal amounts of total protein pooled from about 30 kidneys from each genotype. **F:** Densitometry of bands in the two blots depicted in **E** showing increased total Tie-2 (**open bars**) and phosphorylated Tie-2 (**black bars**) levels in *Ang-2*$^{LZ/LZ}$ kidneys versus *Ang-2*$^{+/+}$ organs. **Bars**: 30 μm, **A** and **B**; 15 μm, **C** and **D**.

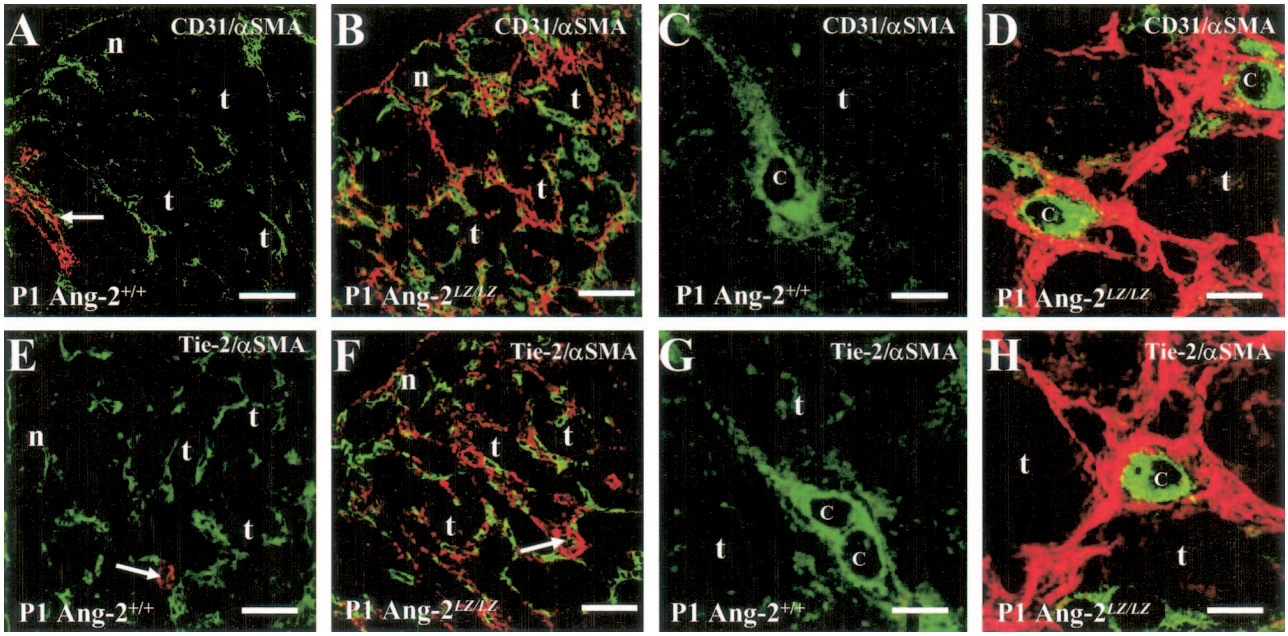

Figure 6. Double-immunofluorescence studies for CD31/αSMA and Tie-2/αSMA. Frames show *Ang-2*$^{+/+}$ (**A**, **C**, **E**, and **G**) and *Ang-2*$^{LZ/LZ}$ (**B**, **D**, **F**, and **H**) P1 littermate kidneys, with data representative of four to five animals of each genotype. **A**, **B**, **E**, and **F** are low-power views of the renal cortex, while **C**, **D**, **G,** and **H** are high-power views. The following structures are indicated: nephrogenic zone (n), cortical tubules (t) just below the nephrogenic zone, arterial vessels (**arrows**), and capillary lumens (c). CD31 and Tie-2 signals appear green and αSMA signals appear red; all frames are from merged images. In both genotypes, CD31 and Tie-2 are detected in the nephrogenic zone and between cortical tubules, and αSMA is detected in walls of arterial vessels. In the *Ang-2*$^{LZ/LZ}$ kidneys, but not in wild-type littermates, αSMA is also clearly immunolocalized between tubules. The high-power views of wild-type kidneys make evident that the endothelial markers, CD31 (**C**) and Tie-2 (**G**), are present in capillaries lacking surrounding αSMA-expressing cells. In contrast, equivalent views of null mutant kidneys show that CD31- (**D**) and Tie-2- (**H**) expressing capillaries are generally surrounded by cells expressing αSMA. Furthermore, there is generally no colocalization of the endothelial and smooth muscle proteins (note that the few yellow "speckles" sometimes detected at the interface of EC and surrounding cells are likely caused by the overlap of processes of the two cell types in the same confocal cut). **Bars:** 60 μm, **A**, **B**, **E**, and **F**; 5 μm, **C**, **D**, **G**, and **H**.

has undergone a non-specific insult, and that the renal interstitial mesenchymal population undergoes an injury reaction. This explanation seems unlikely, however, because αSMA up-regulation was clearly observed in the embryonic period (see Figure 3, A and C) at a time when chylous ascites were absent (data not shown), and also because neonatal mutant kidneys were grossly structurally intact, with no subtle signs of injury such as macrophage infiltration or tubular necrosis. From our double-immunostaining studies, at least some of the αSMA-positive cells in null mutant mice approximated very closely to CD31- and Tie-2-positive interstitial capillaries. We speculate that, if the *Ang-2*$^{LZ/LZ}$ mice were to survive the neonatal period, the former cells may fully differentiate into an aberrant population of pericytes/VSMC and that these cells then might impair the return of reabsorbed tubular filtrate into the circulation. In the future, the study of *Ang-2* null mutant mice in which the lymphatic phenotype is "rescued" by insertion of *Ang-1* into the *Ang-2* locus,[20] might allow prolonged study of the renal lesion and could be informative in testing this hypothesis since such animals do not die in infancy.

As mentioned in the Introduction, pericytes and VSMC fail to differentiate fully in *Ang-1* null mutant mice, which may be attributed to secondary signaling failure between EC and adjacent mesenchymal precursors. Kidney vessel pericytes and VSMC probably have an endogenous origin from renal mesenchymal cells, as assessed by transplantation experiments.[47] During development of diverse organs, pericytes express PDGFRβ, and this receptor is thought to transduce migration and differentiation signals from EC-derived PDGFB.[30,31] Our observations that PDGFRβ is prominently expressed by a subpopulation of cells in the peritubular area of *Ang-2*$^{LZ/LZ}$ kidneys are perhaps consistent with the idea that increased Tie-2 activation by mutant EC might indirectly lead to increased mesenchymal differentiation into pericyte precursors. As outlined in the Introduction, pericytes can also express other proteins, apart from αSMA, such as NG2 and desmin. Our double-immunostaining experiments allowed us to explore expression of these proteins in cells in between cortical tubules. These results suggest that NG2 is normally expressed by peritubular cells and at least some αSMA-positive cells in *Ang-2* null mutants co-express NG2, PDGFRβ and desmin, although the expression pattern of αSMA appeared more spatially extensive than the three other proteins.

Ang-2 is prominently expressed by maturing RA[7,39] but we found no major changes in the morphology of large RA, although we cannot exclude subtle, undetected effects. In the future, it would be interesting to formally assess mutant arteries for expression of genes known to be active in normal maturing RA, such as renin and aquaporin 1.[48,49] Similarly, although *Ang-2* is transiently expressed by differentiating mesangial cells,[7,39] we found no gross anomalies in mutant glomeruli. However, since most glomeruli form and mature in the weeks after birth, the early death of *Ang-2* null mutant mice precludes detailed analysis to assess a putative role for Ang-2 in glomerular differentiation. We speculate that Ang-2 made

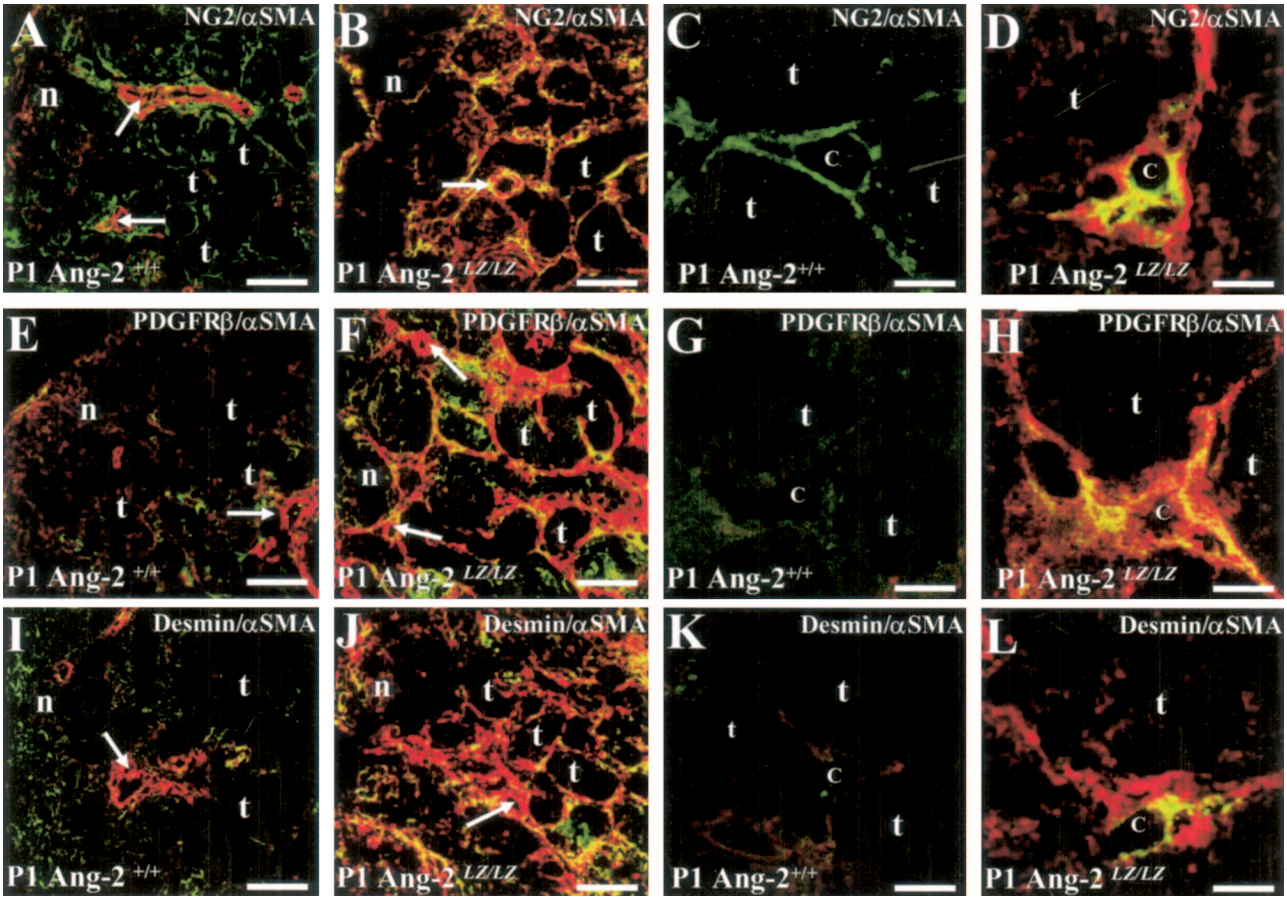

Figure 7. Double-immunofluorescence studies for NG2/αSMA, PDGFRβ/αSMA, and desmin/αSMA. Frames show *Ang-2*$^{+/+}$ (**A**, **C**, **E**, **G**, **I**, and **K**) and *Ang-2*$^{LZ/LZ}$ (**B**, **D**, **F**, **H**, **J**, and **L**) P1 littermate kidneys, with data representative of four to five animals of each genotype. **A**, **B**, **E**, **F**, **I**, and **J** are low-power views of the renal cortex, while **C**, **D**, **G**, **H**, **K**, and **L** are high-power views. The following structures are indicated: nephrogenic zone (n), cortical tubules (t) just below the nephrogenic zone, arterial vessels (**arrows**), and putative capillary lumens (c). NG2, PDGFRβ, and desmin signals appear green and αSMA signals appear red, with co-expressing cells appearing yellow; all frames are from merged images. In both genotypes, αSMA is detected in walls of arterial vessels. In wild-type kidneys, NG2 is expressed by cells between tubules (**A** and **C**), there is a faint PDGFRβ signal between tubules (**E** and **G**), and there is a faint signal for desmin in the nephrogenic cortex (**I**) but not between tubules below the nephrogenic zone (**K**). In null mutant kidneys, peritubular areas express prominent αSMA (**B**, **F**, and **J**); high-power views of *Ang-2*$^{LZ/LZ}$ organs confirm this impression and furthermore, show cells which often co-express the markers NG2 (yellow cells in **D**), PDGFRβ (yellow cells in **H**) and desmin (yellow cells in **L**). **Bars:** 90 μm, **A**, **B**, **E**, **F**, **I**, and **J**; 8 μm in **C**, **D**, **G**, **H**, **K**, and **L**.

by large RA and perhaps mesangial cells may not have major local actions during normal development but instead the factor is secreted into the renal circulation so that Ang-2 would be delivered via efferent glomerular arterioles into cortical peritubular areas. Here, we speculate that the factor may act on differentiating interstitial capillaries. Yuan et al[7,38] observed high Ang-2 expression in postnatal kidneys in descending limbs of loops of Henle and postulated an effect on maintaining the integrity of vasa rectae in the outer medulla. This microcirculation cannot be studied in the current model because *Ang-2*$^{LZ/LZ}$ mice die before the medulla, and the vasa rectae, are properly formed.

Deregulation of survival and growth of the cortical peritubular microcirculation occurs in diverse acquired nephropathies associated with both acute and chronic renal damage (eg, disease induced by toxins, ischemia, or subtotal nephrectomy).[42,50–52] Moreover, in several renal disease models, the integrity of peritubular capillaries has a positive correlation with renal function.[52] For example, in the rat remnant kidney, tubular VEGF-A expression diminishes, correlating with attrition of adjacent capillaries, and the administration of VEGF-A minimizes loss of peritubular capillaries and stabilizes renal function.[52] Renal angiopoietin and Tie gene expression is deregulated in some of these diseases, perhaps indicating that these molecules have active roles in the pathophysiology of these disorders.[50,51] The results of our current study lend further support to the suggestion that deregulation of Ang/Tie signaling might contribute to disorganization of peritubular vessels, and adjacent mesenchymal-like cells, in renal diseases. This contention could, in the future, be investigated by studying the effects of angiopoietin blockade (eg, by soluble Tie receptors) or administration of Ang-1 or Ang-2 in models of acquired renal disease.

Acknowledgments

We thank W. Kriz (University of Heildelberg) for helpful discussion.

References

1. Woolf AS, Yuan HT:. The development of kidney blood vessels. The Kidney: From Normal Development to Congenital Disease. Edited by Vize PD, Woolf AS, Bard JBL. Amsterdam, Elsevier Science/Academic Press, 2003, pp 251–266
2. Robert B, St John PL, Hyink DP, Abrahamson DR: Evidence that embryonic kidney cells expressing flk-1 are intrinsic, vasculogenic angioblasts. Am J Physiol 1996, 271:F744–F753
3. Loughna S, Hardman P, Landels E, Jussila L, Alitalo K, Woolf AS: A molecular and genetic analysis of renal glomerular capillary development. Angiogenesis 1997, 1:84–101
4. Loughna S, Yuan HT, Woolf AS: Effects of oxygen on vascular patterning in Tie1/LacZ metanephric kidneys in vitro. Biochem Biophys Res Commun 1998, 247:361–366
5. Kolatsi-Joannou M, Li X, Suda T, Yuan HT, Woolf AS: Expression and potential role of angiopoietins and Tie-2 in early development of the mouse metanephros. Dev Dyn 2001, 222:120–126
6. Oliver JA, Barasch J, Yang J, Herzlinger D, Al-Awqati G: Metanephric mesenchyme contains embryonic renal stem cells. Am J Physiol 2002, 283:F799–F809
7. Yuan H-T, Suri C, Landon DN, Yancopoulos GD, Woolf AS: Angiopoietin-2 is a site-specific factor in differentiation of mouse renal vasculature. J Am Soc Nephrol 2000, 11:1055–1066
8. Kriz W, Kaissling B: Structural organization of the mammalian kidney. The Kidney. Edited by Seldin DW, Giebisch G. 2000, Raven Press, New York, pp 587–654
9. Kitamoto Y, Tokunaga H, Tomita K: Vascular endothelial growth factor is an essential molecule for mouse kidney development: glomerulogenesis and nephrogenesis. J Clin Invest 1997, 99:2351–2357
10. Gerber HP, Hillan KJ, Ryan AM, Kowalski J, Keller G-A, Rangell L, Wright BD, Radtke F, Aguet M, Ferrara N: VEGF is required for growth and survival in neonatal mice. Development 1999, 126:1149–1159
11. Takahashi T, Takahashi K, Gerety S, Wang H, Anderson DJ, Daniel TO: Temporally compartmentalized expression of ephrin-B2 during renal glomerular development. J Am Soc Nephrol 2001, 12:2673–2682
12. Andres A-C, Munarini N, Djonov V, Bruneau S, Zuercher G, Loercher S, Rohrbach V, Ziemiecki A: EphB4 receptor tyrosine kinase transgenic mice develop glomerulopathies remininscent of aglomerular vascular shunts. Mech Dev 2003, 120:511–516
13. Soriano P: Abnormal kidney development and hematological disorders in PDGF β-receptor mutant mice. Genes Dev 1994, 8:1888–1896
14. Lindhahl P, Hellstrom M, Kalen M, Karlsson L, Pekny M, Pekna M, Soriano P, Betsholtz C: Paracrine PDGF-B/PDGF-Rβ signaling controls mesangial cell development in kidney glomeruli. Development 1998, 125:3313–3322
15. Haas CS, Amann K, Schittny J, Blaser B, Muller U, Hartner A: Glomerular and renal vascular structural changes in α8 integrin-deficient mice. J Am Soc Nephrol 2003, 14:2288–2296
16. Kloth S, Gerdes J, Wanke C, Minuth WW: Basic fibroblast growth factor is a morphogenic modulator in kidney vessel development. Kidney Int 1998, 53:970–978
17. Fierlbeck W, Liu A, Coyle R, Ballermann BJ: Endothelial cell apoptosis during glomerular capillary lumen formation in vivo. J Am Soc Nephrol 2003, 14:1349–1354
18. Suri C, Jones PF, Patan S, Bartunkova S, Maisonpierre PC, Davis S, Sato TN, Yancopoulos GD: Requisite role of angiopoietin-1, a ligand for the TIE2 receptor, during embryonic angiogenesis. Cell 1996, 87:1171–1180
19. Suri C, McClain J, Thurston G, McDonald DM, Zhou H, Oldmixon EH, Sato TN, Yancopoulos GD: Increased vascularization in mice overexpressing angiopoietin-1. Science 1998, 282:468–471
20. Gale NW, Thurston G, Hackett SF, Renard R, Wang Q, McClain J, Martin C, Witte C, Witte MH, Jackson D, Suri C, Campochiaro PA, Wiegand SJ, Yancopoulos GD: Angiopoietin-2 is required for postnatal angiogenesis and lymphatic patterning, and only the latter role is rescued by angiopoietin-1. Dev Cell 2002, 3:411–423
21. Gale NW, Thurston G, Davis S, Wiegand SJ, Holash J, Rudge JA, Yancopoulos GD: Complementary and coordinated roles of the VEGFs and angiopoietins during normal and pathologic vascular formation. Cold Spring Harb Symp Quant Biol 2002, 67:267–273
22. Davis S, Papadopoulos N, Aldrich TH, Mainsonpierre PC, Huang T, Kovac L, Xu A, Leidich R, Radziejewska E, Rafique A, Goldberg J, Jain V, Bailey K, Karow M, Fadnl J, Samuelsson SJ, Goldberg J, Ioffe E, Rudge JS, Daly TJ, Radziejewski C, Yancopoulos GD: Angiopoietins have distinct modular domains essential for receptor binding, dimerization, and superclustering. Nat Struct Biol 2003, 10:38–44
23. Koblizek TI, Weiss C, Yancopoulos GD, Deutsch U, Risau W: Angiopoietin-1 induces sprouting angiogenesis in vitro. Curr Biol 1998, 8:529–532
24. Papapetropoulos A, Garcia-Cardena G, Dengler TJ, Maisonpierre PC, Yancopoulos GD, Sessa WC: Direct actions of angiopoietin-1 on human endothelium: evidence for network stabilization, cell survival, and interaction with other angiogenic growth factors. Lab Invest 1999, 79:213–223
25. Hungerford JE, Little CD: Developmental biology of the vascular smooth muscle cell: building a multilayered vessel wall. J Vasc Res 1999, 36:2–27
26. DeRuiter MC, Poelmann RE, VanMunsteren JC, Mironov V, Markwald RR, Gitternberger-de Groot AC: Embryonic endothelial cells transdifferentiate into mesenchymal cells expressing smooth muscle actins in vivo and in vitro. Circ Res 1997, 80:444–451
27. Witmer AN, van Blijswijk BC, van Noorden CJF, Vrensen JFJM, Schlingemann RO: In vivo angiogenic phenotype of endothelial cells and pericytes induced by vascular endothelial growth factor-A. J Histochem Cytochem 2004, 52:39–52
28. Ozerdem U, Grako KA, Dahlin-Huppe K, Monosov E, Stallcup WB: NG2 proteoglycan is expressed exclusively by mural cells during vascular morphogenesis. Dev Dyn 2001, 222:218–227
29. Collett G, Wood A, Alexander MY, Varnum BC, Boot-Handford RP, Ohanian V, Ohanian J, Fridell YW, Canfield AE: Receptor tyroisne kinase Axl modulates the osteogenic differentiation of pericytes. Circ Res 2003, 92:1123–1129
30. Hellstrom M, Kalen M, Lindahl P, Abramsson A, Betsholtz C: Role of PDGF-B and PDGFR-β in recruitment of vascular smooth muscle cells and pericytes during embryonic blood vessel formation in the mouse. Development 1999, 126:3047–3055
31. Hirschi KK, Rohovsky SA, Beck LH, Smith SR, D'Amore PA: Endothelial cells modulate the proliferation of mural cell precursors via platelet-derived growth factor-BB and heterotypic cell contact. Circ Res 1999, 84:298–305
32. Maisonpierre PC, Suri C, Jones PF, Bartunkova S, Wiegand SJ, Radziejewski C, Compton D, McClain J, Aldrich TH, Papadopoulos N, Daly TJ, Davis S, Sato TN, Yancopoulos GD: Angiopoietin-2, a natural antagonist for Tie2 that disrupts in vivo angiogenesis. Science 1997, 277:55–60
33. Kim I, Kim JH, Moon SO, Kwak HJ, Kim N-G, Koh GY: Angiopoietin-2 at high concentration can enhance endothelial cell survival through the phophatidylinositol 3′-kinase/Akt signal transduction pathway. Oncogene 2000, 19:4549–4552
34. Teichert-Kuliszewska K, Maisonpierre PC, Jones N, Campbell AI, Master Z, Bendeck MP, Alitalo K, Dumont DJ, Yancopoulos GD, Stewart DJ: Biological action of angiopoietin-2 in a fibrin matrix model of angiogenesis is associated with activation of Tie2. Cardiovasc Res 2001, 49:659–670
35. Mochizuki Y, Nakamura T, Kanetake H, Kanda S: Angiopoietin 2 stimulates migration and tube-like structure formation of murine brain capillary endothelial cells through c-Fes and c-Fyn. J Cell Sci 2002, 115:175–183
36. Carlson TR, Feng Y, Maisonpierre PC, Mrksich M, Morla AO: Direct cell adhesion to the angiopoietins mediated by integrins. J Biol Chem 2001, 276:26516–26625
37. Hackett SF, Wiegand S, Yancopoulos G, Campochiaro PA: Angiopoietin-2 plays an important role in retinal angiognesis. J Cell Physiol 2002, 192:182–187
38. Yuan HT, Suri C, Yancopoulos GD, Woolf AS: Expression of angiopoietin-1, angiopoietin-2, and the Tie-2 receptor tyrosine kinase during mouse kidney maturation. J Am Soc Nephrol 1999, 10:1722–1736
39. Yuan HT, Yang SP, Woolf AS: Hypoxia upregulates angiopoietin-2, a Tie-2 ligand, in mouse mesangial cells. Kidney Int 2000, 58:1912–1919
40. Satchell SC, Harper SJ, Tooke JE, Kerjaschki D, Saleem MA, Mathieson PW: Human podocytes express angiopoietin 1, a potential regulator of glomerular vascular endothelial growth factor. J Am Soc Nephrol 2002, 13:544–550

41. Pitera JE, Smith VV, Woolf AS, Milla PJ: Embryonic gut anomalies in a mouse model of retinoic acid-induced caudal regression syndrome: delayed gut looping, rudimentary cecum, and anorectal anomalies. Am J Pathol 2001, 159:2321–2329
42. Yuan HT, Li XZ, Pitera JE, Long DA, Woolf AS: Peritubular capillary loss following mouse acute nephrotoxicity correlates with downregulation of vascular endothelial growth factor-A and hypoxia-inducible factor-1α. Am J Pathol 2003, 163:2289–2301
43. Yancopoulos GD, Davis S, Gale NW, Rudge JS, Wiegand SJ, Holash J: Vascular-specific growth factors and blood vessel formation. Nature 2000, 407:242–248
44. Kriehuber E, Breiteneder-Geleff S, Groeger M, Soleiman A, Schoppmann SF, Stingl G, Kerjaschki D, Maurer D: Isolation and characterization of dermal lymphatic and blood endothelial cells reveal stable and functionally specialized cell lineages. J Exp Med 2001, 194:797–808
45. Kriz W, Dieterich JH: The lymphatic system of the kidney in some mammals: light and electron microscopic investigations. Z Anat Entwicklungsgesch 1970, 13:117–147
46. Hong Y-K, Harvey N, Noh Y-H, Schacht V, Hirakawa S, Detmar M, Oliver G: Prox1 is a master control gene in the program specifying lymphatic endothelial cell fate. Dev Dyn 2002, 225:351–357
47. Sequeira Lopez ML, Pentz ES, Robert B, Abrahamson DR, Gomez RA: Embryonic origin and lineage of juxtaglomerular cells. Am J Physiol 2001, 281:F345–F356
48. Reddi V, Zaglul A, Pentz ES, Gomez RA: Renin-expressing cells are associated with branching of the developing kidney vasculature. J Am Soc Nephrol 1998, 9:63–71
49. Kim J, Kim WY, Han KH, Knepper MA, Nielsen S, Madsen KM: Developmental expression of aquaporin 1 in the rat renal vasculature. Am J Physiol 1999, 276:F498–F509
50. Long DA, Woolf AS, Suda T, Yuan HT: Increased renal angiopoietin-1 expression in folic acid-induced nephrotoxicity in mice. J Am Soc Nephrol 2001, 12:2721–2731
51. Pillebout E, Burtin M, Yuan HT, Briand P, Woolf AS, Friedlander G, Terzi F: Proliferation and remodeling of the peritubular microcirculation after nephron reduction: association with the progression of renal lesions. Am J Pathol 2001, 159:547–560
52. Kang D-H, Kanellis J, Hugo C, Truong L, Anderson S, Kerjaschki D, Schreiner GF, Johnson RJ: Role of the microvascular endothelium in progressive renal disease. J Am Soc Nephrol 2002, 13:806–816